REGULAR PAPER

Effects of GaN cap layer thickness on photoexcited carrier density in green luminescent InGaN multiple quantum wells

Japanese Journal of Applied Physics **62**, 031001 (2023) **REGULAR PAPER**
https://doi.org/**10.35848/1347-4065/acc4fd**

Effects of GaN cap layer thickness on photoexcited carrier density in green luminescent InGaN multiple quantum wells

Hideaki Murotani[1,2*], Keigo Nakatsuru[1], Satoshi Kurai[1], Narihito Okada[1], Yoshiki Yano[3], Shuichi Koseki[3], Guanxi Piao[3], and Yoichi Yamada[1*]

[1]*Department of Electrical and Electronic Engineering, Yamaguchi University, Ube, Yamaguchi 755-8611, Japan*
[2]*Department of Computer Science and Electronic Engineering, National Institute of Technology, Tokuyama College, Shunan, Yamaguchi 745-8585, Japan*
[3]*Taiyo Nippon Sanso Corporation, Tsukuba, Ibaraki 300-2611, Japan*

[*]E-mail: murotani@tokuyama.ac.jp; yamada@yamaguchi-u.ac.jp

Received November 15, 2022; revised March 7, 2023; accepted March 15, 2023; published online April 3, 2023

The effects of GaN cap layers on the optical properties of green luminescent InGaN-based multiple quantum wells were studied by photoluminescence (PL) spectroscopy. The PL peak energy under the selective excitation of the InGaN well layers was lower than that under the band-to-band excitation of the GaN barrier layers. The difference in the PL peak energies between the selective and band-to-band excitations decreased as the cap layer thickness increased, indicating an increase in the nonradiative recombination of photogenerated carriers in the barrier layers. Moreover, the internal quantum efficiency under selective excitation decreased as the cap layer thickness increased because of the increase in the internal electric field strength. © 2023 The Japan Society of Applied Physics

1. Introduction

InGaN-based light-emitting devices are presently the main type of solid-state light sources in the near-UV and blue spectral range.[1,2)] Although the luminescence efficiency of InGaN-based light-emitting devices could still be increased in the green and the longer wavelength range, this improvement is impeded by the difficulty in growing In-rich InGaN/GaN multiple quantum wells (MQWs). Therefore, obtaining In-rich InGaN/GaN MQWs with high optical quality is key to improving the luminescence efficiency.

InGaN/GaN MQWs are difficult to obtain mainly because the In-rich InGaN well layers are difficult to grow due to the large lattice mismatch and low miscibility between GaN and InN.[3)] In addition, the difference in growth temperature between the In-rich InGaN well layers and GaN barrier layers is a further obstacle to obtaining high-quality In-rich InGaN MQWs. Because the In–N bond strength is lower than the Ga–N bond strength, the growth temperature of the In-rich InGaN layers is generally lower than that of the GaN barrier layers; thus, the ambient temperature is increased before the GaN barrier layers are grown. However, increasing the ambient temperature causes In atoms to desorb from the InGaN layers, which decreases the In composition of the InGaN well layers and degrades the interface between the InGaN well and GaN barrier layers.[4,5)]

A method using GaN cap layers and a low growth temperature has been proposed for suppressing the desorption of In atoms from InGaN well layers effectively.[6–11)] Increasing the GaN cap layer thickness lengthens the luminescence wavelength and narrows the luminescence linewidth due to the suppression of the In atom desorption.[7,8)] However, the luminescence intensity decreases as the GaN cap layer thickness increases.[6–8,10,11)] Therefore, to use the GaN cap layers effectively, it is important to understand their effects on the optical properties of InGaN-based MQWs.

Excitation wavelength- and excitation power density-dependent photoluminescence (PL) measurements are powerful techniques for studying the optical properties of MQW systems. These techniques allow the optical properties of the well layer to be evaluated selectively as a function of excitation power density,[12–14)] thereby allowing the effects of GaN cap layers on the optical properties of InGaN well layers to be evaluated selectively. In the present work, we study the effects of GaN cap layers on the PL properties of green luminescent InGaN/GaN MQWs. We conduct excitation power density-dependent PL measurements for InGaN/GaN MQWs with GaN cap layers of different thicknesses under the selective excitation of InGaN well layers and the band-to-band excitation of GaN barrier layers.

2. Experimental procedure

InGaN/GaN MQWs were grown using metalorganic vapor phase epitaxy on a *c*-plane sapphire substrate following the deposition of a 30 nm thick low-temperature GaN buffer layer, a 2.9 μm thick undoped GaN layer, and 10 periods of 1 nm thick InGaN/3 nm thick InGaN strained superlattice layers. Figure 1 shows the schematic of InGaN/GaN MQWs used in the present work. The MQW layer consisted of six periods of a 2.5 nm thick InGaN well layer separated by 6.5 nm thick GaN barrier layers. The surface of the samples was terminated by a 10 nm thick GaN upper barrier layer. The GaN barrier layer comprised a GaN cap layer, a high-temperature GaN layer, and a 1.3 nm thick GaN underlayer for the InGaN well layer. Here, the GaN cap layer was grown directly on each InGaN well layer, and thus the InGaN well layer is sandwiched between the GaN cap layer and the GaN base layer. The GaN cap layer was grown at the same growth temperature as the InGaN well layer in order to suppress the desorption of In atoms from the InGaN well layer. The GaN underlayer was also grown at the same growth temperature as of the InGaN well layer. We prepared three samples with GaN cap layer thicknesses of 0.65, 0.9, and 1.3 nm. for samples A, B, and C, respectively. The total thickness of GaN barrier layers was the same for the samples A, B, and C. These three samples were grown using an identical sequence, excluding the growth times of GaN cap layers and high-temperature GaN layers.

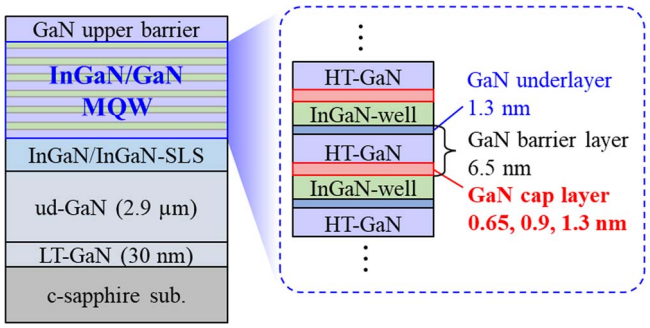

Fig. 1. (Color online) Schematic of InGaN/GaN multiple quantum wells. The 6.5 nm thick GaN barrier layer comprised GaN cap layer (0.65, 0.9, and 1.3 nm), high-temperature GaN layer (4.55, 4.3, and 3.9 nm), and 1.3 nm thick GaN underlayer.

PL measurements were performed using a wavelength-tunable dye laser pumped by a Xe–Cl excimer laser (308 nm) as an excitation source with a pulse width of 20 ns and a repetition rate of 100 Hz. The PL signal was detected by a liquid nitrogen-cooled charge-coupled device camera and a single-grating monochromator having a focal length of 50 cm and a 2400 grooves mm^{-1} grating. The estimated spectral resolution was <0.04 nm (i.e. less than 0.2 meV at approximately 2.4 eV).

3. Experimental results

3.1. PL spectra

Figure 2 shows the PL spectra of three samples at 295 K under an excitation power density of about 10 kW cm^{-2}. The solid and dashed lines indicate the PL spectra taken at excitation wavelengths of 386 and 340 nm, respectively, normalized to the peak intensity of each spectrum. We confirmed that the excitation at wavelengths of 386 and 340 nm corresponded to the selective excitation of the InGaN well layers and the band-to-band excitation of the GaN barrier layers, respectively. The PL band observed around 3.3 eV in the PL spectra of the band-to-band excitation was attributed to the PL from the GaN barrier layers. The PL spectra from the well layers for both the band-to-band and the selective excitations consisted of a single emission band and were accompanied by interference fringes. The PL peak from the well layer under selective excitation (solid lines) was at a lower energy than that under the band-to-band excitation for all samples. The PL peak shifted to a lower energy as the GaN cap layer thickness increased under both the selective and the band-to-band excitations.

Figure 3(a) shows the PL peak energy for both the selective and the band-to-band excitation conditions under an excitation power density of about 10 kW cm^{-2} as a function of GaN cap layer thickness. Because there were nonnegligible interference patterns in the PL spectra, the PL peak energy was estimated by fitting using a Gaussian distribution function. As shown in Fig. 2, the PL peak energy of the band-to-band excitation (closed squares) was higher than that of the selective excitation (closed circles) for all samples, and the PL peak energy decreased as the GaN cap layer thickness increased under both excitation conditions. The decrease in the PL peak energy can be explained by an increase in the In composition of the InGaN well layers. It should be noted that it was difficult to estimate accurately the In composition of the well layers by X-ray diffraction (XRD)

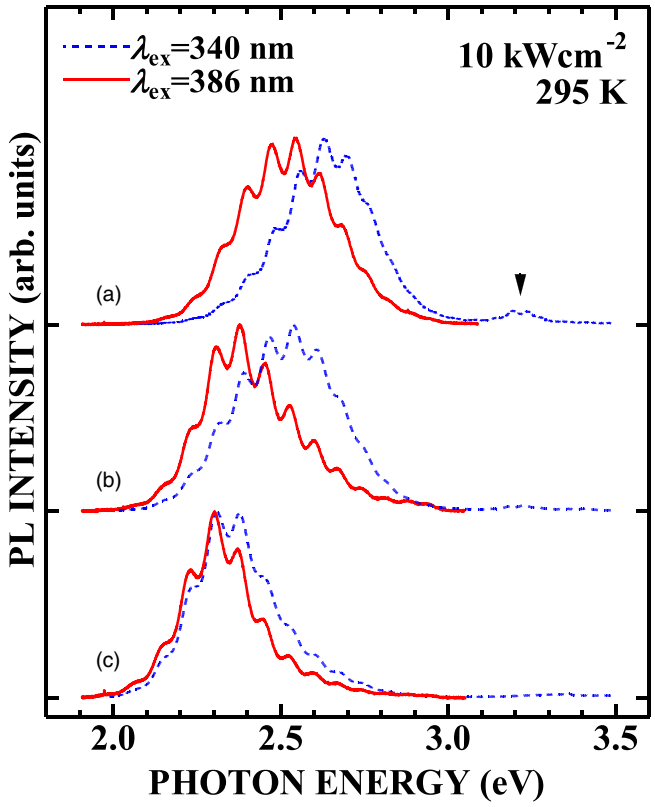

Fig. 2. (Color online) Photoluminescence spectra of samples (a) A, (b) B, and (c) C at 295 K under an excitation power density of about 10^1 kW cm^{-2}. The solid and dashed lines indicate the PL spectra under the selective excitation of InGaN well layers and the band-to-band excitation of GaN barrier layers, respectively.

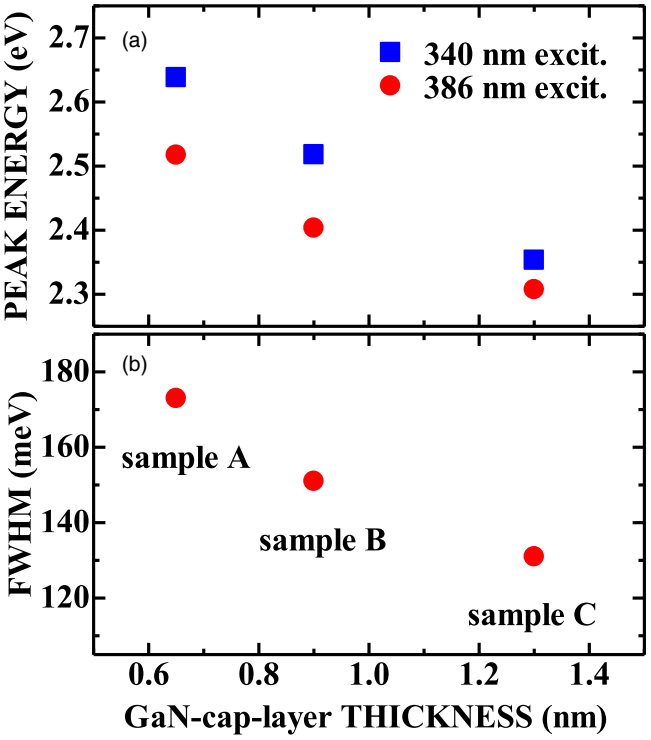

Fig. 3. (Color online) Dependence of photoluminescence (a) peak energy and (b) linewidth (full-width at half maximum) on the GaN cap layer thickness. The closed circles and squares indicate the results under the selective excitation of InGaN well layers and the band-to-band excitation of GaN barrier layers, respectively.

measurements due to the low interfacial abruptness between the well and barrier layers and the overlapping of the XRD patterns of the well layers and InGaN strained superlattice layers.

The energy difference between the PL peaks of the selective excitation and the band-to-band excitation also decreased as the GaN cap layer thickness increased. Figure 3(b) shows the PL linewidth under the selective excitation of the InGaN well layers as a function of the GaN cap layer thickness. The PL linewidths were estimated to be 173, 151, and 131 meV for samples A, B, and C, respectively. That is, the PL linewidth decreased with increasing GaN cap layer thickness, indicating a decrease in the transition energy fluctuation. Thus, the interfacial fluctuation between the well and barrier layers was expected to decrease as the GaN cap layer thickness increased.

3.2. Excitation power–density dependence

Figure 4 shows the excitation power–density dependence of the PL spectra of sample B taken under (a) selective excitation and (b) band-to-band excitation for excitation power densities of about (i) 0.5, (ii) 1.0, (iii) 5.0, (iv) 10, (v) 50, and (vi) 100 kW cm^{-2}. The PL spectra were normalized to the peak intensity of each spectrum. At an excitation power density of 0.5 kW cm^{-2}, the PL peak energy of the selective excitation and the band-to-band excitation were estimated to be 2.375 and 2.401 eV, respectively, and the energy separation of the PL peak energies was estimated to be about 26 meV. The PL spectra under the selective and band-to-band excitations shifted toward the higher-energy side with increasing excitation power density. At an excitation power density of 100 kW cm^{-2}, the PL peak energies of the selective excitation and the band-to-band excitation were about 2.460 and 2.615 eV, respectively, and the energy separation was estimated to be about 155 meV. Thus, the PL blue shift of the band-to-band excitation was greater than that of the selective excitation.

Figure 5(a) shows the excitation power–density dependence of the PL peak energy under selective excitation. The PL peak energy decreased as the GaN cap layer thickness increased over the whole excitation power density range. The PL peak energy was almost constant up to 10^0–10^1 kW cm^{-2}, and then increased with increasing excitation power density for all samples. The blue shift of the PL peak energy was mainly attributed to the gradual screening of the internal electric fields with increasing photoexcited carrier density. The blue shift may also reflect the state-filling effects. The excitation power densities where the slope of PL peak energy with respect to the excitation power density changed from 0 to positive were estimated to be 1.3, 3.2, and 5.2 kW cm^{-2} for samples A, B, and C, respectively, and thus increased with increasing GaN cap layer thickness. The slope of PL peak energy with respect to the excitation power density increased as the GaN cap layer thickness increased, also suggesting an increase in the strength of the internal electric field in the well layers.

Figures 5(b)–5(d) show the PL peak energies of the selective and band-to-band excitations as a function of excitation power density for samples A, B, and C. At higher excitation power densities, the PL peak of the band-to-band excitation (open squares) was higher than that of the selective excitation (closed circles) for all samples. For samples B and C, the PL peak energy of the band-to-band excitation almost agreed with that of the selective excitation at lower excitation

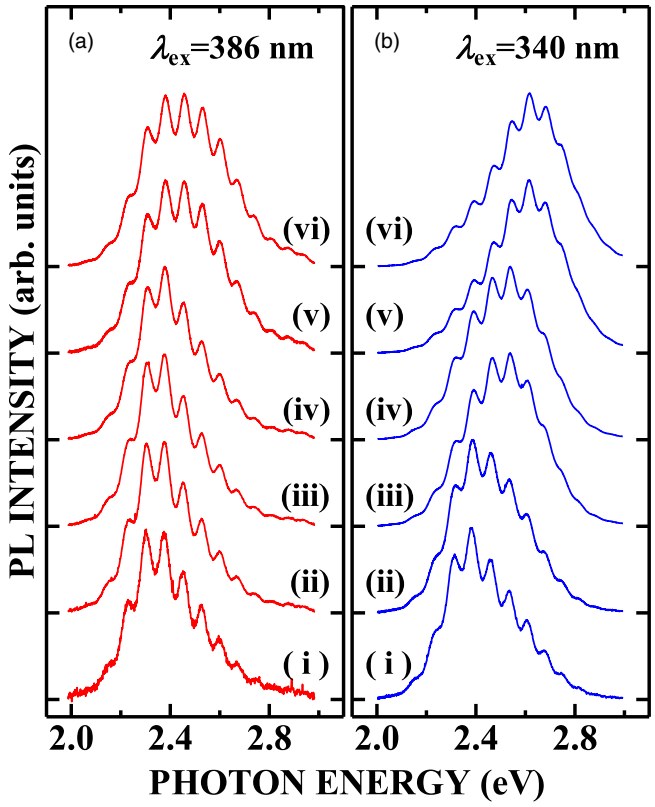

Fig. 4. (Color online) Excitation power–density dependence of photoluminescence spectra under (a) the selective excitation of InGaN well layers and (b) the band-to-band excitation of GaN barrier layers. The excitation power densities are (i) 0.5, (ii) 1.0, (iii) 5.0, (iv) 10, (v) 50, and (vi) 100 kW cm^{-2}.

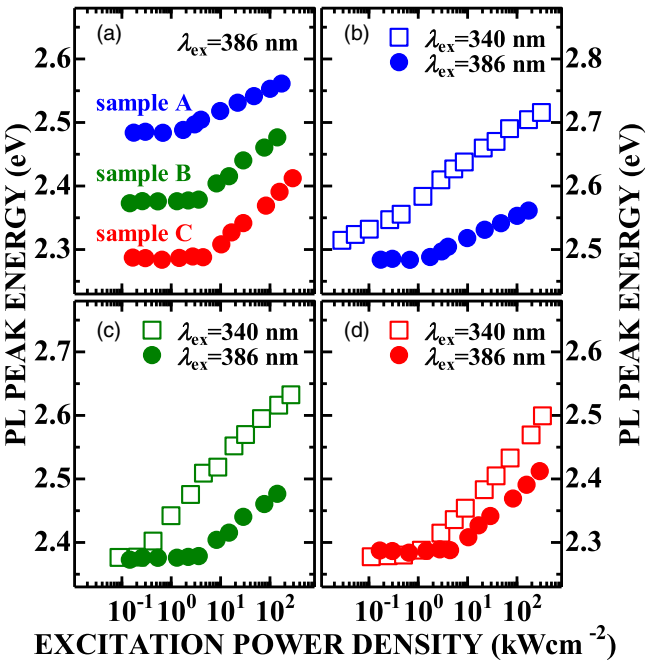

Fig. 5. (Color online) (a) Excitation power–density dependence of the photoluminescence peak energy taken under the selective excitation of InGaN well layers. Comparison of the excitation power–density dependence of photoluminescence peak energy under excitation wavelengths of 386 (closed circles) and 340 nm (open squares) for samples (b) A, (c) B, and (d) C.

power densities. Furthermore, the slopes of the PL peak energy with respect to the excitation power density almost agreed with those for the selective excitation and the band-to-band excitation for all samples. These observations indicated that the difference in the PL peak energy between the selective excitation and the band-to-band excitation reflected the difference in the photoexcited carrier density in the well layers. Thus, these observations also indicated that the photoexcited carrier density under the band-to-band excitation decreased as the GaN cap layer thickness increased.

3.3. Internal quantum efficiency

The internal quantum efficiency (IQE) was evaluated based on the temperature and excitation power density-dependent PL measurements to discuss the effects of the GaN cap layer thickness on luminescence efficiency. To estimate the IQE, the PL efficiency was assumed to be the integrated PL intensity divided by the excitation power density, and was normalized to its maximum value at 10 K. We evaluated the IQE as the normalized PL efficiency.[12,15] Because the photoexcited carrier density under the band-to-band excitation of the GaN barrier layers depended on the GaN cap layer thickness, we evaluated the IQE under the selective excitation of InGaN well layers. The inset in Fig. 6 shows the excitation power–density dependence of IQE at 10, 60, 120, 180, 240, and 295 K for sample A under selective excitation. The IQE increased, and then decreased with increasing excitation power density, even at 10 K. This dependence of IQE was also observed in samples B and C. The increase in the IQE at the lower excitation power densities can be explained by the filling of nonradiative recombination centers.[12,13] Thus, the efficiency curve at 10 K indicated that the nonradiative recombination centers were active even at 10 K under the lower photoexcited carrier density. However, there was no significant change between the efficiency curves at 10 and 60 K under lower excitation power densities. This indicated that the thermal activation of the nonradiative recombination center below 60 K was minor, suggesting that the effects of nonradiative recombination centers were insignificant. Therefore, the assumption that the maximum IQE at 10 K was almost 100% was appropriate in this case.

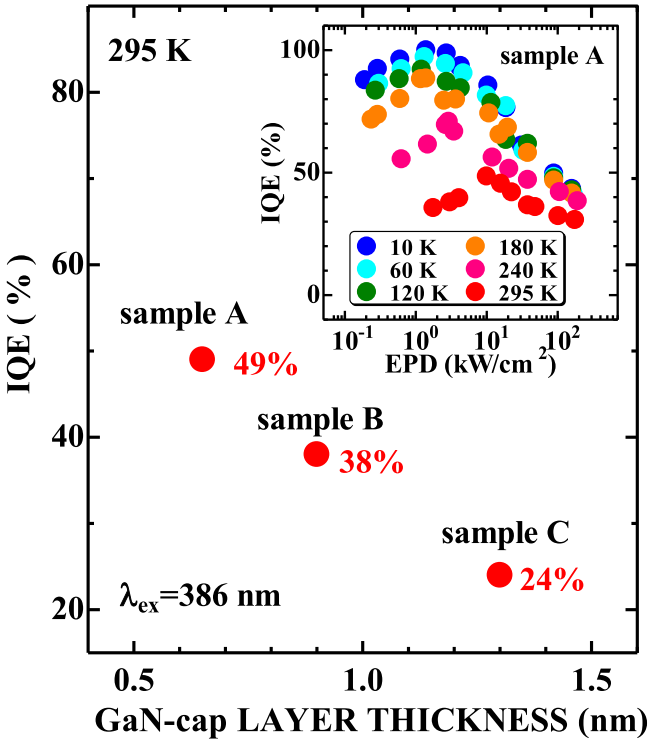

Fig. 6. (Color online) Maximum internal quantum efficiency at 295 K under the selective excitation of InGaN well layers as a function of GaN cap layer thickness. The inset shows the excitation power–density dependence of internal quantum efficiency at 10, 60, 120, 180, 240, and 295 K for sample A.

The decrease in the IQE at higher excitation power densities is known as the "efficiency droop phenomenon." Some possible origins for efficiency droop have been reported, such as Auger recombination of carriers,[16–19] saturation of localized centers and consequent transfer into nonradiative recombination centers,[20–24] and carrier loss via indirect absorption.[25] Although it is difficult to clarify the origin of the decrease in IQE from our observations alone, the efficiency curves for the three samples were similar at higher excitation power densities. This suggested that changes in the GaN cap layer thickness and the associated changes in the quality of the GaN barrier layer did not affect the efficiency droop substantially.

Figure 6 shows the maximum IQE at 295 K under selective excitation as a function of GaN cap layer thickness. The maximum IQE was estimated to be 49% for sample A, 38% for sample B, and 24% for sample C, and decreased as the GaN cap layer thickness increased. This indicated that the changes in GaN cap layer thickness affected the IQE even under the selective excitation of InGaN well layers. The decrease in the IQE reflected the decrease in the radiative recombination rate of photoexcited carriers in the well layers and the increase in the nonradiative recombination rate of the photoexcited carriers. The decrease in the radiative recombination rate is expected to be caused by an increase in the strength of internal electric fields. The increase in nonradiative recombination may be due to the degradation of the GaN barrier layer as the GaN cap layer thickness increased.

4. Discussion

We focus first on the dependence of the PL peak energy of InGaN-based MQWs on the GaN cap layer thickness. The PL peak energy decreased with increasing the GaN cap layer thickness for both the selective excitation and the band-to-band excitation conditions (Fig. 3). The decrease in the PL peak energy can be explained by the decrease in the transition energy due to the decrease in the bandgap energy of the well layers and the increase in the strength of internal electric fields in the well layers.[26–28] The slope of PL peak energy with respect to the excitation power density increased with the GaN cap layer thickness [Figs. 5(b)–5(d)]. The increase in the slope of PL peak energy indicated an increase in the strength of the internal electric fields. Thus, the strength of the internal electric fields in the well layer increased with the GaN cap layer thickness. Although the strength of the internal electric fields depends on the thickness of the well and barrier layers,[29] the thickness of the well layers and the total thickness of the barrier layers, which was the sum of the thicknesses of the GaN underlayer, high-temperature-GaN layer, and GaN cap layer, were the same for all samples. Hence, the increase in the strength of internal electric fields was attributed to the increase in the In composition of the

well layers, which also decreased the bandgap energy of the well layers.

We now discuss the difference in the photoexcited carrier density in the well layers between the selective and the band-to-band excitation conditions. The difference in the PL peak energy between the selective excitation and the band-to-band excitation conditions was attributed to the difference in the photoexcited carrier density in the well layers [Figs. 5(b)–5(d)]. Hence, the difference in the excitation power density at the same PL peak energy between the two excitation conditions corresponded to the difference in the photoexcited carrier density in the well layers. The photoexcited carrier densities of samples A, B, and C for the band-to-band excitation were estimated to be about 200, 30, and 5 times larger than those for the selective excitation, respectively. Assuming that the excitation volume in the MQW region is cylindrical, the excitation volume of the band-to-band excitation was 4.3 times larger than that of the selective excitation for the entire MQW region and 7.6 times larger than that of the selective excitation for the topmost well layer. Thus, the large difference in the photogenerated carrier density of sample A could not be explained by the difference in the excitation volume and reflected mainly the difference in the absorption coefficients between the excitation wavelengths of 340 and 386 nm. That is, the absorption coefficients of the InGaN well and GaN barrier layers for the excitation wavelength of 340 nm were much larger than that of InGaN well layers for the excitation wavelength of 386 nm.

The difference in the photoexcited carrier density between the two excitation wavelengths decreased as the GaN cap layer thickness increased. Although the change in the absorption coefficient of the well layers reflecting the change in the In composition is expected, we consider that the change in the absorption coefficient is not enough to lead to the estimated decrease in the difference. Thus, the decrease in the difference meant that the carrier inflow from the barrier layer into the well layer decreased as the GaN cap layer thickness increased, and the annihilation of photoexcited carriers in the barrier layers was greater in samples with thicker GaN cap layers. Moreover, the ratio of PL intensities from the well layers and the barrier layers in the PL spectra under the band-to-band excitation decreased with increasing GaN cap layer thickness. This indicates that the nonradiative recombination processes in the barrier layers increased with increasing GaN cap layer thickness. Hence, the increase in carrier annihilation in the barrier layers reflected the degradation of the optical quality of the barrier layers with increasing GaN cap layer thickness, and that there were many nonradiative recombination centers in the GaN cap layers,[30,31] which may be due to the low growth temperature. Therefore, our observations suggest that the photoexcited carrier density in the InGaN well layers under band-to-band excitation was strongly affected by the quality of GaN barrier layers and varied by more than two orders of magnitude, even for the same structure.

Finally, we discuss the effects of the GaN cap layer thickness on the IQE of InGaN MQWs. The maximum IQE decreased with increasing GaN cap layer thickness (Fig. 6). This implies a decrease in the radiative recombination rate and an increase in the nonradiative recombination rate with increasing GaN cap layer thickness. Because the strength of the internal electric fields in the well layers increased with the GaN cap layer thickness, the radiative recombination rate should decrease. In addition, the optical quality of GaN barrier layers is expected to degrade with increasing GaN cap layer thickness. The optical quality degradation of the GaN barrier layers may increase the nonradiative recombination rate even under the selective excitation of the InGaN well layers because the penetration of electron and hole wavefunctions into the GaN barrier layers could not be neglected. Therefore, when using a GaN cap layer in InGaN MQWs, it is necessary to design a quantum well structure that takes into account the negative effect of the GaN cap layer.

5. Conclusions

We studied the effects of GaN cap layers on the PL properties of green luminescent InGaN/GaN MQWs. The PL peak energy under the selective excitation of InGaN well layers was lower than that under the band-to-band excitation of GaN barrier layers, reflecting the difference in the photoexcited carrier density in the well layers. The difference in the PL peak energies between the selective and band-to-band excitations decreased with increasing GaN cap layer thickness, indicating the increase in the nonradiative recombination of photogenerated carriers in GaN barrier layers, reflecting the optical quality degradation of the GaN barrier layers. Moreover, the IQE under the selective excitation decreased with increasing GaN cap layer thickness, which also showed the degradation of the GaN barrier layers and the decrease in the radiative recombination rate due to the increase in the internal electric field strength.

Acknowledgments

This work was partially supported by JSPS KAKENHI Grant Nos. JP16H04335, JP16H06428, and JP20K04585.

ORCID iDs

Hideaki Murotani https://orcid.org/0000-0001-9820-9926
Satoshi Kurai https://orcid.org/0000-0002-7561-9583
Yoichi Yamada https://orcid.org/0000-0002-6395-7876

1) S. Nakamura, Rev. Mod. Phys. **87**, 1139 (2015).
2) C. Weisbuch, ECS J. Solid State Sci. Technol. **9**, 016022 (2020).
3) I. Ho and G. B. Stringfellow, Appl. Phys. Lett. **69**, 2701 (1996).
4) Y. Wang, X. J. Pei, Z. G. Xing, L. W. Guo, H. Q. Jia, H. Chen, and J. M. Zhou, J. Appl. Phys. **101**, 033509 (2007).
5) T. Lermer, I. Pietzonka, A. Avramescu, G. Brüderl, J. Müller, S. Lutgen, and U. Strauss, Phys. Status Solidi A **208**, 1199 (2011).
6) Y.-L. Hu et al., Appl. Phys. Lett. **100**, 161101 (2012).
7) S. T. Pendlebury, P. J. Parbrook, D. J. Mowbray, D. A. Wood, and K. B. Lee, J. Cryst. Growth **307**, 363 (2007).
8) J. Yang et al., J. Appl. Phys. **117**, 055709 (2015).
9) Y. Zhu, T. Lu, X. Zhou, G. Zhao, H. Dong, Z. Jia, X. Liu, and B. Xu, Appl. Phys. Express **10**, 061004 (2017).
10) X. Wang, F. Liang, D. Zhao, Z. Liu, J. Zhu, and J. Yang, Nanoscale Res. Lett. **15**, 191 (2020).
11) Y. Zhao, G. Li, S. Zhang, F. Liang, M. Zhou, D. Zhao, and D. Jiang, Opt. Mater. Express **11**, 1411 (2021).
12) T. Kohno, Y. Sudo, M. Yamauchi, K. Mitsui, H. Kudo, H. Okagawa, and Y. Yamada, Jpn. J. Appl. Phys. **51**, 072102 (2012).
13) H. Murotani and Y. Yamada, Jpn. J. Appl. Phys. **58**, 011003 (2019).
14) H. Murotani et al., Jpn. J. Appl. Phys. **58**, SCCB02 (2019).

15) S. Watanabe, N. Yamada, M. Nagashima, Y. Ueki, C. Sasaki, Y. Yamada, T. Taguchi, K. Tadatomo, H. Okagawa, and H. Kudo, Appl. Phys. Lett. **83**, 4906 (2003).
16) Y. C. Shen, G. O. Mueller, S. Watanabe, N. F. Gardner, A. Munkholm, and M. R. Krames, Appl. Phys. Lett. **91**, 141101 (2007).
17) K. T. Delaney, P. Rinke, and C. G. Van de Walle, Appl. Phys. Lett. **94**, 191109 (2009).
18) E. Kioupakis, P. Rinke, K. T. Delaney, and C. G. Van de Walle, Appl. Phys. Lett. **98**, 161107 (2011).
19) J. Iveland, L. Martinelli, J. Peretti, J. S. Speck, and C. Weisbuch, Phys. Rev. Lett. **110**, 177406 (2013).
20) B. Monemar and B. E. Sernelius, Appl. Phys. Lett. **91**, 181103 (2007).
21) X. A. Cao, Y. Yang, and H. Guo, J. Appl. Phys. **104**, 093108 (2008).
22) J. Hader, J. V. Moloney, and S. W. Koch, Appl. Phys. Lett. **96**, 221106 (2010).
23) S. Hammersley, D. Watson-Parris, P. Dawson, M. J. Godfrey, T. J. Badcock, M. J. Kappers, C. McAleese, R. A. Oliver, and C. J. Humphreys, J. Appl. Phys. **111**, 083512 (2012).
24) M. J. Davies, T. J. Badcock, P. Dawson, M. J. Kappers, R. A. Oliver, and C. J. Humphreys, Appl. Phys. Lett. **102**, 022106 (2013).
25) E. Kioupakis, P. Rinke, A. Schleife, F. Bechstedt, and C. G. Van de Walle, Phys. Rev. B **81**, 241201 (2010).
26) T. Takeuchi, S. Sota, M. Katsuragawa, M. Komori, H. Takeuchi, H. Amano, and I. Akasaki, Jpn. J. Appl. Phys. **36**, L382 (1997).
27) T. Takeuchi, C. Wetzel, S. Yamaguchi, H. Sakai, H. Amano, I. Akasaki, Y. Kaneko, S. Nakagawa, Y. Yamaoka, and N. Yamada, Appl. Phys. Lett. **73**, 1691 (1998).
28) L.-H. Peng, C.-W. Chuang, and L.-H. Lou, Appl. Phys. Lett. **74**, 795 (1999).
29) V. Fiorentini, F. Bernardini, F. Della Sala, A. Di Carlo, and P. Lugli, Phys. Rev. B **60**, 8849 (1999).
30) S. M. Olaizola, S. T. Pendlebury, J. P. O'Neill, D. J. Mowbray, A. G. Cullis, M. S. Skolnick, P. J. Parbrook, and A. M. Fox, J. Phys. D **35**, 599 (2002).
31) J. Liu, Z. Li, L. Zhang, F. Zhang, A. Tian, K. Zhou, D. Li, S. Zhang, and H. Yang, Appl. Phys. Express **7**, 111001 (2014).